AFRL-RX-WP-TP-2011-4418

AGILE THERMAL MANAGEMENT STT-RX
Catalytic influence of Ni-based additives on the dehydrogentation properties of ball milled MgH2 (PREPRINT)

Patrick J. Shamberger, Jonathan E. Spowart, and Andrey A. Voevodin
Thermal Sciences & Materials Branch

Placidus B. Amama and John T. Grant
University of Dayton Research Institute

Timothy S. Fisher
Purdue University

DECEMBER 2011

AIR FORCE RESEARCH LABORATORY
MATERIALS AND MANUFACTURING DIRECTORATE
WRIGHT-PATTERSON AIR FORCE BASE, OH 45433-7750
AIR FORCE MATERIEL COMMAND
UNITED STATES AIR FORCE

NOTICE AND SIGNATURE PAGE

Using Government drawings, specifications, or other data included in this document for any purpose other than Government procurement does not in any way obligate the U.S. Government. The fact that the Government formulated or supplied the drawings, specifications, or other data does not license the holder or any other person or corporation; or convey any rights or permission to manufacture, use, or sell any patented invention that may relate to them.

This report was cleared for public release by the USAF 88th Air Base Wing (88 ABW) Public Affairs Office and is available to the general public, including foreign nationals. Copies may be obtained from the Defense Technical Information Center (DTIC) (http://www.dtic.mil).

AFRL-RX-WP-TR-2011-4418 HAS BEEN REVIEWED AND IS APPROVED FOR PUBLICATION IN ACCORDANCE WITH ASSIGNED DISTRIBUTION STATEMENT.

//SIGNED//

KARLA STRONG, Program Manager
Thermal Sciences and Materials Branch
Nonmetallic Materials Division

//SIGNED//

NADER HENDIZADEH, Chief
Thermal Sciences and Materials Branch
Nonmetallic Materials Division

//SIGNED//

SHASHI K. SHARMA, Deputy Chief
Nonmetallic Materials Division
Materials and Manufacturing Directorate

This report is published in the interest of scientific and technical information exchange, and its publication does not constitute the Government's approval or disapproval of its ideas or findings.

*Disseminated copies will show "//signature//" stamped or typed above the signature blocks.

REPORT DOCUMENTATION PAGE

Form Approved
OMB No. 0704-0188

1. REPORT DATE *(DD-MM-YY)*	2. REPORT TYPE	3. DATES COVERED *(From - To)*
December 2011	Technical Paper	1 December 2011 – 1 December 2011

4. TITLE AND SUBTITLE

AGILE THERMAL MANAGEMENT STT-RX
Catalytic influence of Ni-based additives on the dehydrogentation properties of ball milled MgH2 (PREPRINT)

5a. CONTRACT NUMBER
In-house

5b. GRANT NUMBER

5c. PROGRAM ELEMENT NUMBER
62102F

6. AUTHOR(S)

Patrick J. Shamberger, Jonathan E. Spowart, and Andrey A. Voevodin (AFRL/RXBT)
Placidus B. Amama and John T. Grant (University of Dayton Research Institute)
Timothy S. Fisher (Purdue University)

5d. PROJECT NUMBER
4347

5e. TASK NUMBER
62

5f. WORK UNIT NUMBER
BT110100

7. PERFORMING ORGANIZATION NAME(S) AND ADDRESS(ES)

Nonmetallic Materials Division
Thermal Sciences& Materials Branch
Air Force Research Laboratory, Materials and Manufacturing Directorate
Wright-Patterson Air Force Base, OH 45433-7750
Air Force Materiel Command, United States Air Force

University of Dayton Research Institute
Purdue University

8. PERFORMING ORGANIZATION REPORT NUMBER
AFRL-RX-WP-TP-2011-4418

9. SPONSORING/MONITORING AGENCY NAME(S) AND ADDRESS(ES)

Air Force Research Laboratory
Materials and Manufacturing Directorate
Wright-Patterson Air Force Base, OH 45433-7750
Air Force Materiel Command
United States Air Force

10. SPONSORING/MONITORING AGENCY ACRONYM(S)
AFRL/RXBT

11. SPONSORING/MONITORING AGENCY REPORT NUMBER(S)
AFRL-RX-WP-TP-2011-4418

12. DISTRIBUTION/AVAILABILITY STATEMENT
Approved for public release; distribution unlimited.

13. SUPPLEMENTARY NOTES
The U.S. Government is joint author of this work and has the right to use, modify, reproduce, release, perform, display, or disclose the work. PA Case Number and clearance date: 88ABW-2010-6732, 29 Dec 2010. Preprint journal article to be submitted to Journal of Materials Research. This document contains color. © Materials Research Society 2011.

14. ABSTRACT

The catalytic influence of Ni, Zr_2Ni_5, and $LaNi_5$ on the dehydrogenation properties of milled MgH_2, was investigated. MgH_2 milled in the presence of Ni (5wt%) and Zr_2Ni_5 (5wt%) catalysts for 2 h showed apparent activation energies, E_A, of 81 and 79 kJ/mo1, respectively, corresponding to ~50% decrease in E_A and a moderate decrease (~100 °C) in the decomposition temperature (T_{dec}). A further 27 °C decrease in T_{dec} was observed after milling with 10 wt% Ni. Based on the E_A values, the catalytic activity decreased in the following order: Ni ~ Zr_2Ni_5 > $LaNi_5$. X-ray photoelectron spectroscopy analysis of the milled and dehydrogenated states of the hydrides modified with Ni catalyst revealed that the observed reduction in E_A may be due to the ability of Ni catalyst to decrease the amount of oxygen atoms in defective positions that are capable of blocking catalytically active sites thereby enhancing the dehydrogenation kinetics. In particular, our results reveal a strong correlation between the type of oxygen species absorbed on Ni-modified MgH_2 and E_A of the dehydrogenation reaction.

15. SUBJECT TERMS
magnesium hydride, MgH, thermal energy storage materials, endothermic reaction

16. SECURITY CLASSIFICATION OF:			17. LIMITATION OF ABSTRACT:	NUMBER OF PAGES	19a. NAME OF RESPONSIBLE PERSON (Monitor) / 19b. TELEPHONE NUMBER *(Include Area Code)*
a. REPORT	b. ABSTRACT	c. THIS PAGE			
Unclassified	Unclassified	Unclassified	SAR	14	Karla Strong / N/A

Catalytic influence of Ni-based additives on the dehydrogenation properties of ball milled MgH_2

Placidus B. Amama[a] and John T. Grant
Air Force Research Laboratory, Materials and Manufacturing Directorate, RXB, Wright-Patterson AFB, Ohio 45433; and University of Dayton Research Institute (UDRI), University of Dayton, Dayton, Ohio 45469

Jonathan E. Spowart, Patrick J. Shamberger, and Andrey A. Voevodin
Air Force Research Laboratory, Materials and Manufacturing Directorate, RXB, Wright-Patterson AFB, Ohio 45433

Timothy S. Fisher
Air Force Research Laboratory, Materials and Manufacturing Directorate, RXB, Wright-Patterson AFB, Ohio 45433; and School of Mechanical Engineering, Purdue University, West Lafayette, Indiana 47907; and Birck Nanotechnology Center, Purdue University, West Lafayette, Indiana 47907

(Received 1 March 2011; accepted 11 July 2011)

The catalytic influence of Ni, Zr_2Ni_5, and $LaNi_5$ on the dehydrogenation properties of milled MgH_2 was investigated. MgH_2 milled in the presence of Ni (5 wt%) and Zr_2Ni_5 (5 wt%) catalysts for 2 h showed apparent activation energies, E_A, of 81 and 79 kJ/mol, respectively, corresponding to ~50% decrease in E_A and a moderate decrease (~100 °C) in the decomposition temperature (T_{dec}). A further 27 °C decrease in T_{dec} was observed after milling with 10 wt%Ni. Based on the E_A values, the catalytic activity decreased in the following order: Ni ≈ Zr_2Ni_5 > $LaNi_5$. X-ray photoelectron spectroscopy analysis of the milled and dehydrogenated states of the hydrides modified with Ni catalyst revealed that the observed reduction in E_A may be due to the ability of Ni catalyst to decrease the amount of oxygen atoms in defective positions that are capable of blocking catalytically active sites thereby enhancing the dehydrogenation kinetics. In particular, our results reveal a strong correlation between the type of oxygen species adsorbed on Ni-modified MgH_2 and the E_A of the dehydrogenation reaction.

I. INTRODUCTION

The development of new and efficient thermal energy storage (TES) materials remains a major challenge in addressing needs in a variety of areas from intermittent solar energy harvesting to thermal management of transient, high-flux heat loads. Conceivable TES application temperatures could range from near room temperature (for cooling electronics, for example) to moderate temperatures commensurate with "temperature lift" heat pumping cycles and waste heat recovery from power generation cycles. The latter temperatures could fall in the range of several hundred degrees Celsius. A variety of passive materials have been developed and used for TES including paraffin waxes, water tanks, and low-capacity reversible metal hydrides, among others. Paraffin wax has been used as a TES medium for decades.[1–4] The current state-of-the-art packaging technology for containing and conducting heat to paraffin wax reduces its effective heat storage density at the system level appreciably. Other material systems of possible interest are summarized in Table I; notably, paraffins, salts, and liquid metals have impractically low inherent enthalpies of phase change when normalized by mass. In fact, the only two example materials that exceed 1 MJ/kg are water (liquid–vapor) and a metal hydride. Regarding water, the slow kinetics of boiling/evaporation, limited largely by the nucleation, ebullition, and departure time of ~10 ms for each bubble,[5] and the requirement for handling large quantities of vapor make it less practical.

Metal hydrides offer a potential materials solution, enabled by the uniquely high formation enthalpy of hydrogen gas, as well as other advantages such as on-demand cooling, fast thermal response, and system designs that are compact and lightweight.[6] However, they also offer significant challenges to be overcome. First, we note that not all metal hydrides have high-energy storage capacities (cf., $LaNi_5H_6$ as shown in Table I). In fact, some well-known intermetallic metal hydrides have been studied recently for reversible and reasonably fast thermal storage,[6] but the low thermal energy density of such "classical" hydrides renders them poorly suited for high-density thermal storage. However, some metal hydrides do offer exceptionally high TES density. For instance, a reaction of Mg and H_2 can be used to store thermal energy, and a theoretical energy density of 2.81 MJ/kg is possible.[7] Magnesium hydride (MgH_2) is a well-studied

[a]Address all correspondence to this author.
e-mail: Placidus.Amama@wpafb.af.mil
DOI: 10.1557/jmr.2011.230

TABLE I. Inherent material enthalpy of phase change and/or reaction for candidate thermal storage materials at temperatures between 100 and 400 K.

Material	ΔH (MJ/kg)
Metal hydride: MgH_2 (solid–vapor, with reaction)	2.81
Water (liquid–vapor)	2.25
Water (solid–liquid)	0.33
Metal hydride: $LaNi_5H_6$ (solid–vapor, with reaction)	0.23
Paraffin waxes (solid–liquid)	0.20–0.25
Low melting point metals and alloys (solid–liquid)	0.01–0.08
Hydrous salts (solid–liquid)	0.05–0.3
Inorganic salts (solid–liquid)	0.01–0.4

example,[8–11] but the high temperatures required for hydrogen release and sluggish kinetics make it impractical for highly peaked input rate TES applications. The broader metal hydride research community has been very active recently in developing new hydrides for hydrogen storage for fuel cell operations, but in that application low reaction enthalpies are desired because high reaction enthalpies decrease overall efficiency and create severe cooling problems upon hydrogenation (i.e., fueling).[11] Because of the emphasis on hydrogen storage for fuel cell vehicles, pure metal hydrides with high heats of reaction have been largely neglected in recent research compared to those with moderate-to-low reaction heats. Conversely, our work focuses on metal hydrides that offer extraordinarily high inherent thermal storage capacity, while also exploring new routes for controllable kinetics enhancement and high effective thermal conductivity. However, accessing this large thermal density under rapid heating conditions required for projected applications, efficient heat flow, reduced desorption temperatures, and fast chemical kinetics of candidate hydrides like MgH_2 are required; therefore, new material enhancement through improved catalysis are required.

Hydrogen gas produced from a metal hydride offers exceptionally good thermal transport properties. For example, the electrical power generation industry uses hydrogen extensively (often produced by on-site electrolysis) to provide high-rate cooling of turbine generator windings.[12] The use of hydrogen for such massive-scale cooling is in concert with its high thermal properties, viz, thermal conductivity, $\kappa_{th} = 0.18$ W/mK; specific heat, $C_p = 14.21$ kJ/kg·K; and specific gas constant, $R = 4.12$ kJ/kg·K. The typical thermophysical properties of hydrogen are an order of magnitude superior to those of other common reactive gases such as NH_3, CO_2, steam (H_2O), and air. Only inert He gas approaches the thermal performance of hydrogen. Furthermore, hydrogen's high specific gas constant makes it uniquely suitable for rapid isothermal gas expansion cooling, which suggests additional utility beyond TES.

Motivated by the overall benefits of generating H_2 from metal hydrides for polymer electrolyte membrane fuel cells, many research efforts have focused on substantially improving the hydrogen storage properties of metal hydrides using different approaches such as mechanical ball milling, doping with catalysts, confinement in nanoporous scaffolds, and reactions with metals, nonmetals, or metal hydrides.[11,13–16] In general, nanostructuring via mechanical ball milling[16] or wet chemistry methods[17] and the use of suitably tailored catalysts as dopants[18] have shown the most promise. A variety of transition metal and metal oxide catalytic additives (Ni, Nb, TiO_2, Cu, Co, Fe, etc) have been investigated under various conditions.[19–22] In summarizing the available literature, we note that nickel-catalyzed MgH_2 reactions have shown better dehydrogenation properties in comparison to other transition metal catalysts[11,23,24]; the high catalytic activity of Ni is attributed to its efficiency in the cleavage of hydrogen bonds during hydrogenation and recombination of hydrogen atoms during dehydrogenation.[11] The reactivity of any given catalyst can be substantially altered by alloying. Although mechanically milled MgH_2–$LaNi_5$[25,26] and MgH_2–Zr_xNi_y[27] composites have been studied separately, a comprehensive comparative study of the hydrogen storage properties of milled MgH_2–$LaNi_5$, MgH_2–Zr_xNi_y, and MgH_2–Ni composites under similar conditions is still lacking, given that all the aforementioned samples were modified differently and dehydrogenation reactions performed at different vacuum levels. As pointed out by Varin et al.,[11] desorption tests of MgH_2 with additives conducted in vacuum are of very limited value because the use of vacuum systems in practical applications of hydrides will greatly complicate the whole design. Therefore, we present herein a comprehensive comparison of the dehydrogenation properties of MgH_2 milled with Ni and Ni alloys. This work also provides further insights into the role of the active catalyst during the dehydrogenation reaction of MgH_2.

II. EXPERIMENTAL SECTION

A. Sample preparation

MgH_2, $LaNi_5$, and Zr_2Ni_5 powders (hydrogen-storage grade) were purchased from Sigma-Aldrich (St. Louis, MO), whereas Ni metal nanopowder ($\leq$100 nm in size and 99.9% in purity) was purchased from American Elements (Los Angeles, CA). The as-received hydrides and catalyst–hydride mixtures were ball milled in a SPEX SamplePrep 8000M Mixer/Mill [high-energy shaker (vibratory) mill], which combines strong shearing and impact forces to mix, blend, and reduce particle size. The clamp movement of the mill is 5.9 cm back-and-forth and 2.5 cm side-to-side, whereas the clamp speed is 1060 cycles per minute. The hydrides were milled in a 65-cm^3 stainless steel vial using 15 stainless steel grinding balls (0.7 cm in diameter) under Ar environment. The ball-to-powder

weight ratio was 13:1, which falls at the lower end of the recommended range of 10–100.[11] The milling time of the as-received hydrides were 1, 2, 5, and 10 h, whereas the catalyst compositions investigated were 2, 5, and 10 wt% and were milled for 2 h except where otherwise stated. Samples were handled in an Ar glove box with the amount of oxygen and water vapor present being less than 10 and 0.1 ppm, respectively, to reduce oxidation and/or hydroxide formation.

B. Differential scanning calorimetry and thermogravimetry (DSC/TGA)

DSC/TGA measurements were performed using a Simultaneous DSC–TGA instrument (SDT 2960 TA Instruments, New Castle, DE). All measurements were carried out with 5–10 mg of sample at atmospheric pressure and repeated to ensure reproducibility. The temperature was linearly increased from room temperature (~25 °C) to 500 °C at a rate of 5 °C/min in a stream of Ar (~50 sccm) to reduce oxidation. The apparent activation energy, E_A, of the dehydrogenation reactions was determined using the Kissinger method. The Kissinger equation[28] given in Eq. (1) is used to obtain information about the kinetics and the reaction order of simple decomposition reactions by analyzing the sensitivity of the decomposition temperature (T_{dec}) to the heating rate (β):

$$\frac{\mathrm{d}\ln\left(\frac{\beta}{T_{max}^2}\right)}{\mathrm{d}\left(\frac{1}{T_{max}}\right)} = -\frac{E_A}{R} \quad , \qquad (1)$$

where R represents the gas constant; E_A is determined from a linear plot of $\ln\frac{\beta}{T^2}$ versus $\frac{1000}{T}$.

The heating rates used for this analysis were 5, 10, and 20 °C/min. Detailed description and assumptions inherent in the Kissinger method are reported in Ref. 28 The TA Universal Analysis software was used to determine the onset temperature (T_{onset}) and T_{dec} after each experiment.

C. Structural transformation and microstructure

Phase identity and purity were characterized by x-ray diffraction (XRD) using a Rigaku D-5000 (Rigaku, Tokyo, Japan) with Cu Kα radiation (λ = 0.15418 nm) operated at 40 kV and 150 mA at room temperature. The scan range was from 2-theta = 20–90°, and the scan rate was 3°/min at a step size of 0.05°. The microstructure of the samples was studied using an FEI Quanta environmental field emission scanning electron microscope (FESEM, FEI, Hillsboro, OR). All images were captured under high vacuum with an accelerating voltage of 20 kV. Backscatter electron imaging allowed differentiation between relatively high atomic mass catalysts and low atomic mass MgH_2. This distinction was confirmed by energy-dispersive spectroscopy, which correlated high backscatter (i.e., bright) regions with high catalyst concentrations.

D. X-ray photoelectron spectroscopy (XPS)

The role of Ni catalyst during the dehydrogenation of MgH_2 was studied via XPS using a Kratos Ultra XPS system (Kratos, Kanagawa, Japan) with a monochromatic Al Kα source ($h\upsilon$ = 1486.6 eV) operated at 12 kV and 10 mA. Samples were loaded on the holders in the glove box and transported in sealed bags to reduce contamination from oxygen and water vapor. The Kratos XPS is equipped with a heating stage in the outer sample treatment chamber (STC) (vacuum level ~2.0×10^{-7} Torr during heating). Samples were placed in the STC and heated to 250 °C at a rate of ~50 °C/min and maintained at this temperature while H_2 desorption was monitored using a residual gas analyzer. After dehydrogenation, the sample was transferred under vacuum to the analysis chamber for spectral acquisition. All samples were analyzed before and after the dehydrogenation process. The C 1s peak (binding energy = 284.8 eV) was used as charge reference for energy calibration. Spectral analysis was performed using CasaXPS software. Least square fitting of the spectra was performed using mixed Gaussian–Lorentzian peaks in the quantification process.

III. RESULTS AND DISCUSSION

A. Optimization of the high-energy ball milling process

The XRD patterns of the MgH_2 in the as-received condition and after ball milling for 1, 2, 5, and 10 h are presented in Fig. 1. The observed reflections of the as-received MgH_2 correspond to tetragonal β-MgH_2 and some retained Mg. After milling for 1 h, there is a structural transformation of the β-MgH_2 to the (metastable) orthorhombic γ-MgH_2 and the formation of MgO. Detailed explanations for the formation of the metastable polymorph and MgO after milling have been provided by Huot et al.[29] All the milled samples exhibit broad peaks—suggesting the formation of nanograins—and prolonged milling up to 10 h did not change the composition of the polymorphs significantly compared to 1-h milling. These XRD observations are generally consistent with previous work[11,16] except that in our work the β–γ transformation occurred after 1 h. In previous studies such as that by Varin et al.,[16] milling for 10 h or longer was required to transform β-MgH_2 to γ-MgH_2. Thus, the high-energy milling process used in the current study appears to be more efficient in generating the metastable γ phase even with a lower-than-typical ball-to-powder weight ratio of 13:1.

The effect of high-energy milling for different durations on the T_{dec} of MgH_2 was studied to optimize the milling conditions. As shown in Fig. 2, the DSC profiles

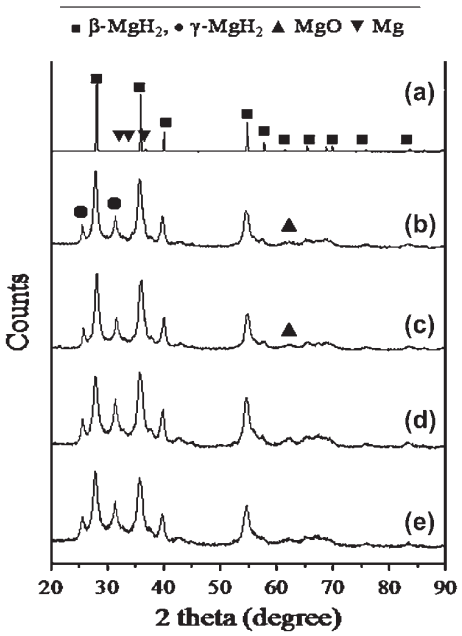

FIG. 1. X-ray diffraction (XRD) patterns showing the microstructural evolution during high-energy milling: (a) as-received MgH_2, (b) 1-h milling, (c) 2-h milling, (d) 5-h milling, and (e) 10-h milling. Phase assignments are made on the basis of comparisons with PDF data.

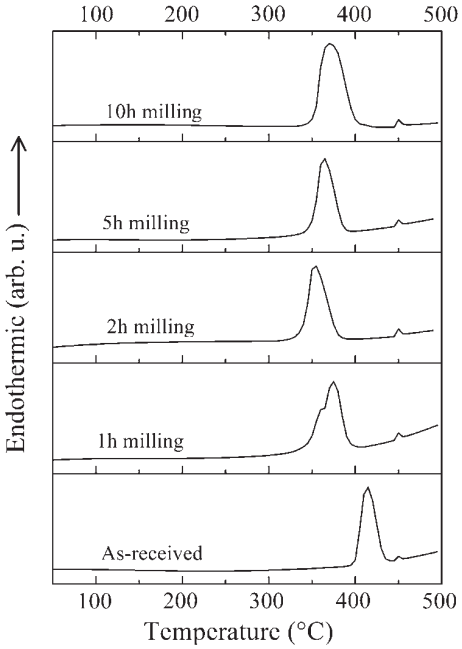

FIG. 2. Differential scanning calorimetry (DSC) profiles of as-received MgH_2 as a function of ball milling duration (heating rate 5 °C/min).

are characterized by a single endothermic peak, which corresponds to the decomposition of the hydride. The T_{dec} (peak maximum temperature) of the as-received MgH_2 sample occurs at 414 °C, whereas the T_{dec} for samples milled for 1, 2, 5, and 10 h are 374, 353, 363, and 371 °C, respectively. A summary of the desorption properties of MgH_2 modified with the different catalysts is presented in Table II. It is believed that the small endothermic peak at 450 °C is an experimental artifact. The reduction of T_{dec} by ~62 °C while maintaining about the same DSC peak area or hydrogen storage capacity implies that the optimum milling time under these conditions is 2 h. Other workers have reported that a reduction in T_{dec} by up to 60 °C typically requires prolonged milling. For instance, Varin et al.[16] reported a reduction in T_{dec} in the range of 40–60 °C for the as-received MgH_2 after milling for 10–100 h. The decrease in T_{dec} after milling is generally attributed to the formation of nanograins, introduction of lattice strains, and phase transformation of tetragonal β-MgH_2 to orthorhombic γ-MgH_2 as confirmed by XRD (Fig. 1).[11,16,29] The FESEM data (not shown) revealed that the as-received MgH_2 has a grain size of ~10 μm, and fine grains are formed with increasing milling time. It is thought that the motion of the balls in the high-energy vibratory mill combines strong shearing and impact forces in various proportions to increase the free energy of the system by increasing surface area and creating lattice defects.[29] No Fe contamination was observed (0.1 at.% detection limit) during XPS analysis of the milled samples suggesting that the reduction in T_{dec} observed is completely due to the milling of the hydride, not from the leaching of Fe from the stainless steel vial or milling tools as observed by Ares et al.[30]

B. Influence of Ni-based catalysts

Further, we examined the dehydrogenation reaction of MgH_2 milled with 2 and 5 wt% of Ni alloys for 2 h. Figure 3 shows the DSC results of the as-received MgH_2, milled MgH_2, and MgH_2 doped with 2 wt% Zr_2Ni_5, $LaNi_5$, and Ni catalysts. The onset temperature (T_{onset}) and T_{dec} for the various samples are summarized in Table II. The T_{onset} represents the point at which the onset tangent line intersects with the baseline of the DSC peak. The DSC results reveal a reduction in T_{dec} due to the catalytic effect of Ni and the Ni alloys, compared to the T_{dec} of MgH_2 milled for 2 h without catalyst. These results are consistent with a similar shift in T_{dec} observed in the TGA profile. The catalytic effect of Ni appears to be marginally higher than for Zr_2Ni_5 or $LaNi_5$ because T_{dec} for the former is 324 °C, whereas the latter are 331 and 333 °C, respectively. Also, the DSC results for MgH_2 milled with Zr_2Ni_5 and $LaNi_5$ exhibit a shoulder near 350 °C, which corresponds to the T_{dec} of MgH_2 milled in the absence of a catalyst. This suggests that unlike pure Ni, the Ni alloys do not seem to catalyze the dehydrogenation reaction completely. Hanada et al.[31] showed that the hydrogen desorption properties of Nb_2O_5-catalyzed MgH_2 are improved with increasing milling time in contrast to that of Ni-catalyzed MgH_2. In our case, the shoulder observed at 350 °C did not disappear

TABLE II. Summary of the dehydrogenation properties of all the catalysts studied.

Samples	Catalyst amount (wt%)	Milling time (h)	Onset temperature, T_{onset} (°C)	Decomposition temperature[a], T_{dec} (°C)	Weight loss[b] (wt%)
MgH_2[c]	–	–	402	414	7.0
MgH_2	–	1	355	374	7.2
MgH_2	–	2	341	353	7.1
MgH_2	–	5	351	363	7.1
MgH_2	–	10	353	371	7.2
MgH_2/Zr_2Ni_5	2	2	306	331	7.0
$MgH_2/LaNi_5$	2	2	311	333	6.8
MgH_2/Ni	2	2	306	324	6.6
MgH_2/Zr_2Ni_5	5	2	293	318	6.5
$MgH_2/LaNi_5$	5	2	289	317	7.1
MgH_2/Ni	5	2	304	323	7.2
MgH_2/Zr_2Ni_5	10	2	286	311	6.2
$MgH_2/LaNi_5$	10	2	281	307	6.0
MgH_2/Ni	10	2	258	287	6.1

[a]Data obtained from differential scanning calorimetry profiles.
[b]Data obtained from thermogravimetry profiles.
[c]As-received MgH_2.

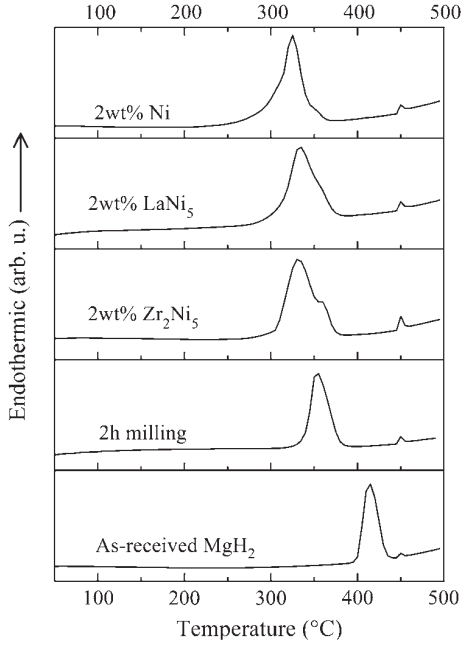

FIG. 3. DSC profiles for the as-received MgH_2, milled MgH_2 (2 h), and MgH_2 milled with 2 wt% Zr_2Ni_5, $LaNi_5$, and Ni catalysts for 2 h (heating rate 5 °C/min).

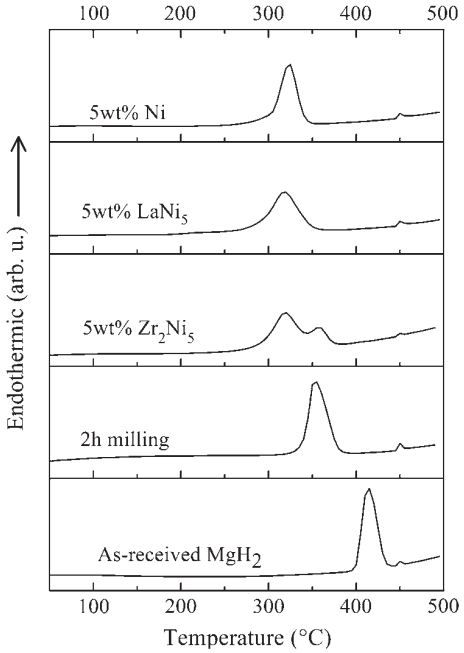

FIG. 4. DSC profiles for the as-received MgH_2, milled MgH_2 (2 h), and MgH_2 milled with 5 wt% Zr_2Ni_5, $LaNi_5$, and Ni catalysts for 2 h each (heating rate 5 °C/min).

with longer milling time (5 h). It should be noted that the T_{dec} values reported here are higher than those obtained from studies performed in vacuum such as that by Hanada et al.[31]

The influence on milling MgH_2 with higher amounts of Ni-based catalysts (5 wt%) was also studied. Figure 4 shows the DSC profiles of the as-received MgH_2, milled MgH_2, and MgH_2 doped with 5 wt% Zr_2Ni_5, $LaNi_5$, and Ni catalysts. The DSC profile of MgH_2 samples milled with Zr_2Ni_5 shows a double desorption peak at ~319 and ~350 °C suggesting that Zr_2Ni_5 does not catalyze the entire reaction. As shown in Fig. 4, the maximum of the endothermic peak is further reduced by ~10 °C upon increasing the catalyst amount from 2 to 5 wt%. High-energy milling of the as-received MgH_2 with 5wt% Ni or Zr_2Ni_5 has therefore resulted in ~100 °C decrease in T_{dec}. Generally, longer milling time (>2 h) did not result in better desorption properties for MgH_2 milled with catalysts. FESEM studies revealed that the large as-received MgH_2 particles were transformed into small grains with sizes ranging from 0.3 to 1 μm, and that the catalyst particles are fairly well-dispersed on the

surface of MgH_2 after 2 h of milling as shown by the representative FESEM image in Fig. 5. The catalytic enhancement of hydrides has been widely demonstrated[11]; however, most studies involve several hours of ball milling. For example, Yonkeu et al.[32] showed that 80 h of ball milling was needed to decrease the T_{dec} of MgH_2 from 429.2 to 368.3 °C using 2 mol% of the body-centered cubic alloy $TiV_{1.1}Mn_{0.9}$ as catalyst. We should note that for studies performed in vacuum, T_{dec} of modified MgH_2 in the range of 200–280 °C with a good rate is common while at 0.1 Mpa H_2, no desorption occurs below 325 °C.[11] Although the T_{dec} achieved at the current stage of our work is still higher than the desired range for TES, the substantial decrease in T_{dec} achieved after only 2 h of milling is noteworthy. Further downshift of T_{dec} may be obtained by improving catalyst dispersion, catalyst–hydride interaction via high-energy wet chemical milling process.

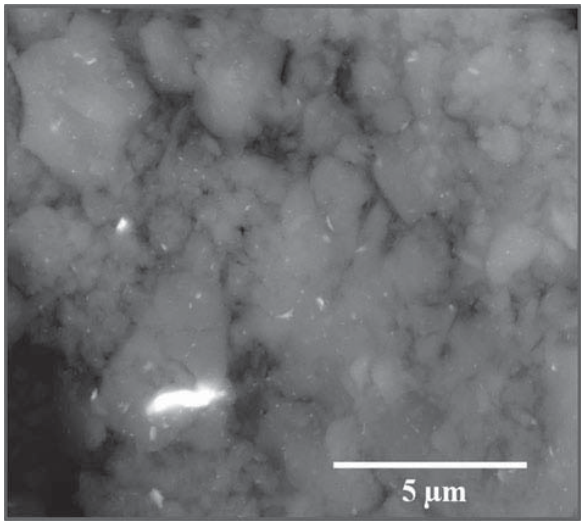

FIG. 5. Backscattered electron micrograph of MgH_2 modified with 5 wt% Ni catalyst. Dispersed lighter areas correspond to Ni-rich phases.

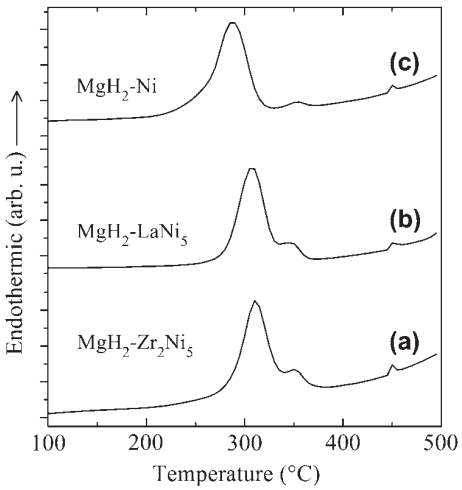

FIG. 7. DSC profiles for MgH_2 milled with 10 wt% (a) Zr_2Ni_5, (b) $LaNi_5$, and (c) Ni catalysts for 2 h each (heating rate 5 °C/min).

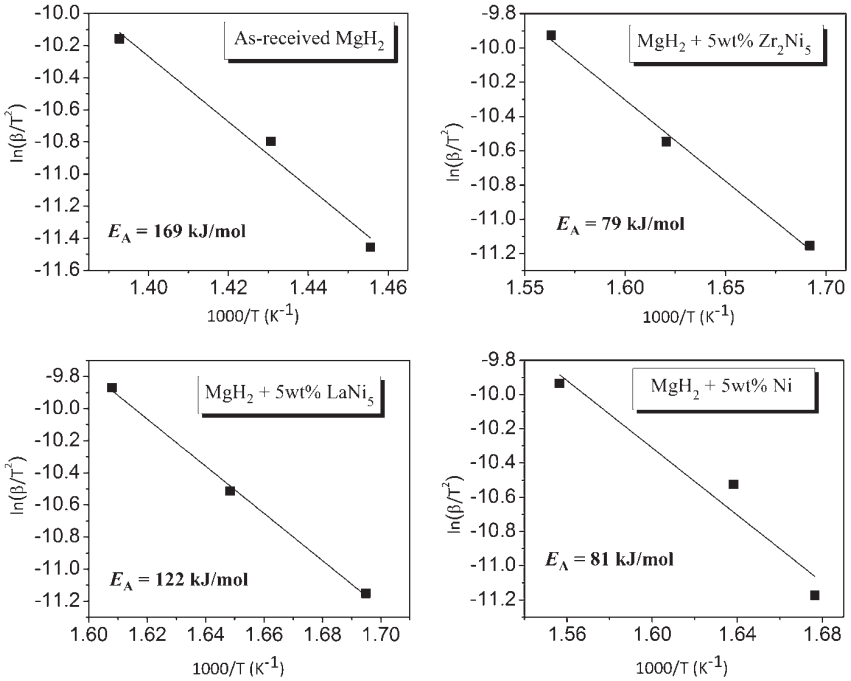

FIG. 6. Kissinger plots for dehydrogenation of as-received MgH_2, MgH_2 milled with 5 wt% Zr_2Ni_5, $LaNi_5$, and Ni catalysts for 2 h each. The heating rates used were 5, 10, and 20 °C/min.

The effect of Ni-based catalysts on the dehydrogenation kinetics of MgH_2 was also investigated. The apparent activation energies, E_A, were determined using the Kissinger method as previously discussed (Fig. 6). The apparent E_A for the as-received MgH_2 is ~169 kJ/mol, which is in agreement with E_A obtained from the Arrhenius plot (E_A = ~168 kJ/mol) for MgH_2 powder purchased from ABCR GmbH & Co. (Karlsruhe, Germany).[11] The apparent E_A for the dehydrogenation reactions of MgH_2 catalyzed by Zr_2Ni_5, $LaNi_5$, and Ni are 79, 122, and 81 kJ/mol, respectively. From the E_A values, it is clear that modifying MgH_2 with Zr_2Ni_5 or Ni catalysts via high-energy milling improves the kinetics significantly; the E_A is reduced by half. It has been shown that milling MgH_2 with nano-Ni particles for 15 min and 20 h reduces the desorption temperature at atmospheric pressure from 418 to 243 and 302 °C, respectively.[11] The apparent E_A of desorption of MgH_2 milled with nanosized Ni for 15 min and micrometer-sized Ni particles for 20 h were 92 and 105 kJ/mol, respectively. The E_A values obtained in our work using Ni and Zr_2Ni_5 particles are comparable to these values.

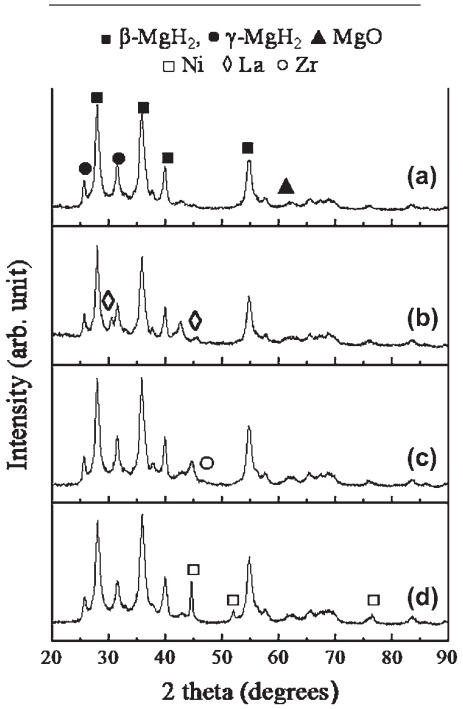

FIG. 8. Powder XRD of (a) milled MgH_2 for 2 h and MgH_2 milled with 10 wt% (b) $LaNi_5$, (c) Zr_2Ni_5 and (d) Ni for 2 h.

Based on the positive effect of the catalysts on T_{dec} and E_A, higher amounts of catalysts were also milled with the as-received MgH_2 for 2 h. The DSC profiles of MgH_2 milled with 10 wt% Zr_2Ni_5, $LaNi_5$, and Ni are shown in Fig. 7. The T_{dec} for MgH_2 milled with 10 wt% Zr_2Ni_5, $LaNi_5$, and Ni were 311, 307, and 287 °C, whereas their T_{onset} were 286, 281, and 258 °C, respectively. Further decrease in T_{dec} was observed after milling with 10 wt% catalyst. In comparison to the as-received MgH_2, the total decrease in T_{dec} was greater than 100 °C for all the samples. The apparent E_A obtained from the Kissinger method for MgH_2 milled with 10 wt% Zr_2Ni_5, $LaNi_5$, and Ni are 85, 97, and 87 kJ/mol, respectively. The apparent E_A does not seem to change significantly with higher catalyst amount except in the case of $LaNi_5$. As the catalyst amount milled with the hydride increases, the H_2 weight penalty during dehydrogenation of the hydride increases, and this does not seem to be severe as evidenced by their respective TGA data (Table II). The weight loss analysis was restricted to the temperature range where MgH_2 undergoes its enthalpy change (>250 °C).

To explore possible structural change due to the increased amount of catalyst, XRD patterns of MgH_2 + 10 wt% catalyst composites were acquired and the results are shown in Fig. 8. It is clear from the observed reflections that the samples are composed of mixtures of the two main polymorphs (β-MgH_2 and γ-MgH_2) and the various catalyst components. In comparison to the XRD pattern of the as-received MgH_2 (Fig. 1), the diffraction peaks of these

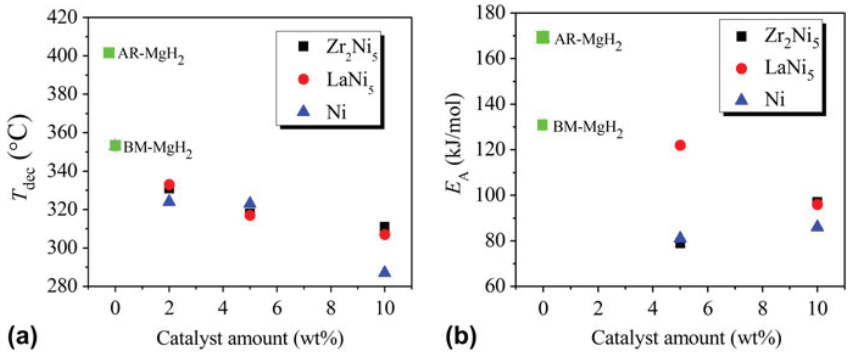

FIG. 9. Effect of milling and the amount of the various catalysts on the decomposition temperature (T_{dec}) and apparent activation energy (E_A) during the dehydrogenation of MgH_2. For comparison, data for as-received MgH_2 (AR-MgH_2) and MgH_2 milled for 2 h (BM-MgH_2) are also included.

composites (Fig. 8) are considerably broadened indicating the formation of nanocrystallites or residual strain. The absence of MgH_2Ni, a common alloy formed when a high amount of Ni is milled with MgH_2 indicates that solid state reactions between the catalyst and MgH_2 may not have occurred.

A summary of the effects of milling and the amounts of Ni, $LaNi_5$, and Zr_2Ni_5 catalysts on T_{dec} and apparent E_A is presented in Figs. 9(a) and 9(b). It is clear from this result that ball milling may have both thermodynamic and kinetic effects—it decreases the T_{dec} from 414 to 353 °C and the E_A from 169 to 131 kJ/mol. The effect of the catalysts on T_{dec} appears to be the same for MgH_2 samples milled with 2 and 5 wt% catalysts; however, Ni catalyst clearly shows the highest downshift of T_{dec} for MgH_2 samples milled with higher catalyst amount (10 wt%). As mentioned earlier, milling MgH_2 with 5 wt% Ni and Zr_2Ni_5 results in improved kinetics, corresponding to ~50% decrease in E_A compared to the as-received MgH_2. Interestingly, increasing the catalyst amount to 10 wt% does not result in a corresponding increase in the dehydrogenation kinetics of MgH_2 samples milled with Ni and Zr_2Ni_5; on the other hand, improved kinetics is observed for MgH_2 milled with 10 wt% $LaNi_5$ possibly due to the increasing active Ni component in the sample.

C. XPS analysis of the role of catalyst

To obtain further insight into the role of the active catalyst (Ni) during the dehydrogenation of MgH_2, XPS analysis was

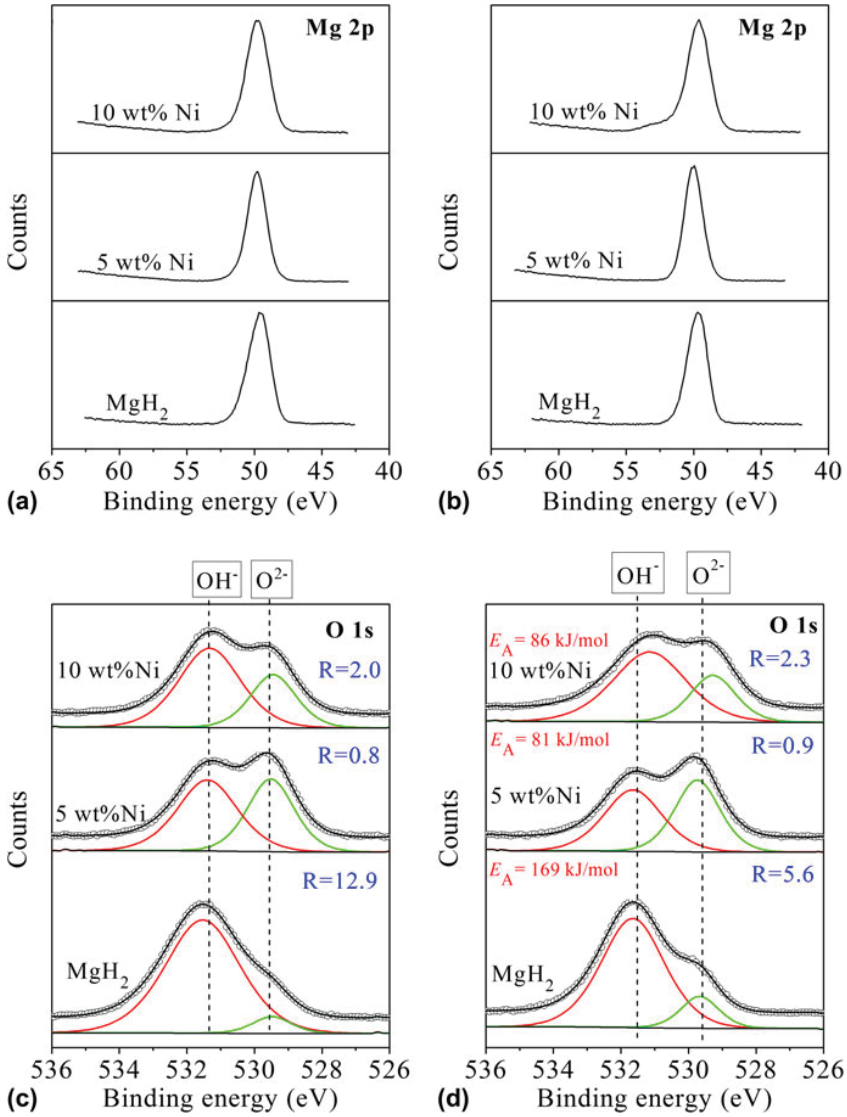

FIG. 10. X-ray photoelectron spectroscopic spectra of as-received MgH_2 and MgH_2 milled with 5 and 10 wt% Ni catalysts: (a) Mg 2p region before reaction, (b) Mg 2p region after reaction, (c) O 1s region before reaction, and (d) O 1s region after reaction. $R = OH^-/O^{2-}$ ratio.

carried out on MgH_2 in the as-received and dehydrogenated states and for MgH_2 + 5 wt% Ni and MgH_2 + 10 wt% Ni in the milled and dehydrogenated states. The XPS spectra of O 1s and Mg 2p regions for the various samples are presented in Fig. 10. The Ni 2p spectra of MgH_2 + 5 wt% Ni exhibited poor signal-to-noise due to the low concentration of Ni. However, the Ni 2p spectra of MgH_2 + 10 wt% Ni showed improved signal-to-noise (not shown), and the binding energies of the $2p_{3/2}$ and $2p_{1/2}$ for the milled hydride state were centered at 852.3 and 869.5 eV and for the dehydrogenated state at 852.1 and 869.5 eV, respectively. The Ni $2p_{3/2}$ and $2p_{1/2}$ peak positions and line shapes are characteristic of metallic Ni,[33] and the peak positions for the milled and dehydrogenated states are somewhat similar indicating that Ni remains in the metallic state during the dehydrogenation of MgH_2. The Mg 2p peaks for all the milled and dehydrogenated states were centered ~50 eV [Figs. 10(a) and 10(b)], consistent with the core level binding energy of Mg in hydrides.[34] The addition of Ni catalyst does not seem to affect the shape and peak position of the Mg 2p peaks. On the other hand, all the O 1s spectra showed doublets indicating that oxygen atoms are present in two different chemical environments [Figs. 10(c) and 10(d)]. The low-binding energy peak is ascribed to O^{2-} or lattice MgO oxygen atoms, whereas the high binding energy (HBE) peak is still unclear but widely associated with hydroxide, hydroxyl, oxygen containing species acting as precursors to support oxide growth or catalytic poison.[35,36] In fact, prior work has shown that the presence of these oxygen species with HBE peak on Ti-based alloy surfaces can block catalytically active sites and prevent H_2 dissociation.[37] Curve fitting of the O 1s spectra using a mixture of Gaussian (50%) and Lorentzian (50%) line shapes to achieve the best fit allowed for the quantification of the oxide and hydroxide components. The ratio of the hydroxyl : oxide (OH^-/O^{2-}) decreases significantly after milling MgH_2 with 5 wt% Ni catalyst suggesting that the presence of Ni decreases the hydroxide component. It should be noted that milling with higher catalyst amount (10 wt% Ni) did not result in further decrease of the OH^-/O^{2-} ratio. Based on the analysis of the O 1s spectra for the different samples and their corresponding E_A data, we hypothesize that there is a strong correlation between the type of oxygen species adsorbed on Ni-modified MgH_2 and the reaction kinetics of the dehydrogenation reaction. Lower OH^-/O^{2-} ratios generally have lower E_A values and vice versa.

IV. CONCLUSIONS

This work has shown that the presence of Ni and Ni alloys in MgH_2 decreases the energy barrier of MgH_2 dehydrogenation, and catalytic activity follows the following order: Ni $\approx$ Zr_2Ni_5 > $LaNi_5$. Using a combination of a high-energy vibrating mill and Ni-based catalysts, we have successfully reduced the T_{dec} of MgH_2 by over 120 °C, from ~414 to ~287 °C. MgH_2 milled for 2 h with Ni (5 wt%) and Zr_2Ni_5 (5 wt%) showed an E_A of 81 and 79 kJ/mol, respectively, corresponding to a ~50% decrease in E_A. These improvements were achieved after only 2 h of milling indicating the efficiency of our high-energy milling procedure. In particular, the XPS data indicate that the milling of MgH_2 with Ni catalyst decreases the amount of oxygen atoms in defective positions that are associated with poisoning of the catalytically active centers, thereby enhancing the dehydrogenation process. This insight into the role of Ni catalyst during the dehydrogenation of MgH_2 would benefit current efforts aimed at improving the hydrogen and heat storage properties of hydrides. Although these results are promising, significant reductions in T_{dec} are desired for many thermal storage applications; therefore, additional ways of improving the surface area density of the hydride grains, catalyst dispersion, and catalyst–hydride interaction are being explored.

ACKNOWLEDGMENTS

Support from the Air Force Research Laboratory and the Air Force Office of Scientific Research are gratefully acknowledged. The authors are grateful to Dr. Karla L. Strong for valuable discussions.

REFERENCES

1. Y. Cai, Q. Wei, F. Huang, S. Lin, F. Chen, and W. Gao: Thermal stability, latent heat and flame retardant properties of the thermal energy storage phase change materials based on paraffin/high density polyethylene composites. *Renew. Energy* **34**, 2117 (2009).
2. J.A. Molefi, A.S. Luyt, and I. Krupa: Investigation of thermally conducting phase-change materials based on polyethylene/wax blends filled with copper particles. *J. Appl. Polym. Sci.* **116**, 1766 (2010).
3. P.C. Stryker and E.M. Sparrow: Application of a spherical thermal conductivity cell to solid n-eicosane paraffin. *Int. J. Heat Mass Transfer* **33**, 1781 (1990).
4. J. Zhang, T.S. Fisher, P.V. Ramachandran, J.P. Gore, and I. Mudawar: A review of heat transfer issues in hydrogen storage technologies. *J. Heat Transfer* **127**, 1391 (2005).
5. V.P. Carey: *Liquid-Vapor Phase-Change Phenomena* (Hemisphere Publishing Corporation, Washington, DC, 1992).
6. C. Park, X. Tang, K.J. Kim, J. Gottschlich, and Q. Leland: Metal hydride heat storage technology for directed energy weapon systems, in *Proceedings of International Mechanical Engineering Congress & Exposition (IMECE2007-42831)*, Vol. 961, November 10–16, 2007, p. 9.
7. A. Reiser, B. Bogdanovic, and K. Schlichte: The application of Mg-based metal-hydrides as heat energy storage systems. *Int. J. Hydrogen Energy* **25**, 425 (2000).
8. M. Tanniru, H.Y. Tien, and F. Ebrahimi: Study of the dehydrogenation behavior of magnesium hydride. *Scr. Mater.* **63**, 58 (2010).
9. L. George and S.K. Saxena: Structural stability of metal hydrides, alanates and borohydrides of alkali and alkali-earth elements: A review. *Int. J. Hydrogen Energy* **35**, 5454 (2010).
10. B. Sakintuna, F. Lamari-Darkrim, and M. Hirscher: Metal hydride materials for solid hydrogen storage: A review. *Int. J. Hydrogen Energy* **32**, 1121 (2007).

11. R.A. Varin, T. Czujko, and Z.S. Wronski: *Nanomaterials for Solid State Hydrogen Storage* (Springer, New York, 2009).
12. S. Nagano, T. Kitajima, K. Yoshida, Y. Kazao, Y. Kabata, D. Murata, and K. Nagakura: Development of world's largest hydrogen-cooled turbine generator, in *Power Engineering Society Summer Meeting, IEEE*, Vol. 2, July 25, 2002, pp. 657–663.
13. D.L. Croston, D.M. Grant, and G.S. Walker: The catalytic effect of titanium oxide based additives on the dehydrogenation and hydrogenation of milled MgH_2. *J. Alloy. Comp*. **492**, 251 (2010).
14. M. Polanski and J. Bystrzycki: The influence of different additives on the solid-state reaction of magnesium hydride (MgH_2) with Si. *Int. J. Hydrogen Energy* **34**, 7692 (2009).
15. J.J. Vajo, S.L. Skeith, and F. Mertens: Reversible storage of hydrogen in destabilized $LiBH_4$. *J. Phys. Chem. B* **109**, 3719 (2005).
16. R.A. Varin, T. Czujko, and Z. Wronski: Particle size, grain size and gamma-MgH_2 effects on the desorption properties of nanocrystalline commercial magnesium hydride processed by controlled mechanical milling. *Nanotechnology* **17**, 3856 (2006).
17. S.B. Kalidindi and B.R. Jagirdar: Highly monodisperse colloidal magnesium nanoparticles by room temperature digestive ripening. *Inorg. Chem*. **48**, 4524 (2009).
18. W. Grochala and P.P. Edwards: Thermal decomposition of the non-interstitial hydrides for the storage and production of hydrogen. *Chem. Rev*. **104**, 1283 (2004).
19. R.A. Varin, T. Czujko, E.B. Wasmund, and Z.S. Wronski: Catalytic effects of various forms of nickel on the synthesis rate and hydrogen desorption properties of nanocrystalline magnesium hydride (MgH_2) synthesized by controlled reactive mechanical milling (CRMM). *J. Alloy. Comp*. **432**, 217 (2007).
20. J. Huot, J.F. Pelletier, L.B. Lurio, M. Sutton, and R. Schulz: Investigation of dehydrogenation mechanism of MgH_2-Nb nanocomposites. *J. Alloy. Comp*. **348**, 319 (2003).
21. N. Hanada, T. Ichikawa, and H. Fujii: Catalytic effect of nanoparticle 3d-transition metals on hydrogen storage properties in magnesium hydride MgH_2 prepared by mechanical milling. *J. Phys. Chem. B* **109**, 7188 (2005).
22. J. Mao, Z. Guo, X. Yu, H. Liu, Z. Wu, and J. Ni: Enhanced hydrogen sorption properties of Ni and Co-catalyzed MgH_2. *Int. J. Hydrogen Energy* **35**, 4569 (2010).
23. W.N. Yang, C.X. Shang, and Z.X. Guo: Site density effect of Ni particles on hydrogen desorption of MgH_2. *Int. J. Hydrogen Energy* **35**, 4534 (2010).
24. L. Xie, Y. Liu, X. Zhang, J. Qu, Y. Wang, and X. Li: Catalytic effect of Ni nanoparticles on the desorption kinetics of MgH_2 nanoparticles. *J. Alloy. Comp*. **482**, 388 (2009).
25. G. Liang, J. Huot, S. Boily, A. Van Neste, and R. Schulz: Hydrogen storage in mechanically milled Mg-$LaNi_5$ and MgH_2-$LaNi_5$ composites. *J. Alloy. Comp*. **297**, 261 (2000).
26. T. Spassov, P. Delchev, P. Madjarov, M. Spassova, and T. Himitliiska: Hydrogen storage in Mg-10áat.% $LaNi_5$ nanocomposites, synthesized by ball milling at different conditions. *J. Alloy. Comp*. **495**, 149 (2010).
27. Z. Dehouche, H.A. Peretti, S. Hamoudi, Y. Yoo, and K. Belkacemi: Effect of activated alloys on hydrogen discharge kinetics of MgH_2 nanocrystals. *J. Alloy. Comp*. **455**, 432 (2008).
28. H.E. Kissinger: Reaction kinetics in differential thermal analysis. *Anal. Chem*. **29**, 1702 (1957).
29. J. Huot, G. Liang, S. Boily, A. Van Neste, and R. Schulz: Structural study and hydrogen sorption kinetics of ball-milled magnesium hydride. *J. Alloy. Comp*. **293–295**, 495 (1999).
30. J.R. Ares, K.F. Aguey-Zinsou, T. Klassen, and R. Bormann: Influence of impurities on the milling process of MgH_2. *J. Alloy. Comp*. **434–435**, 729 (2007).
31. N. Hanada, T. Ichikawa, and H. Fujii: Catalytic effect of Ni nanoparticle and Nb oxide on H-desorption properties in MgH_2 prepared by ball milling. *J. Alloy. Comp*. **404–406**, 716 (2005).
32. A.L. Yonkeu, I.P. Swainson, J. Dufour, and J. Huot: Kinetic investigation of the catalytic effect of a body centered cubic-alloy $TiV_{1.1}Mn_{0.9}$ (BCC) on hydriding/dehydriding properties of magnesium. *J. Alloy. Comp*. **460**, 559 (2008).
33. C.D. Wagner, A.V. Naukim, A. Kraut-Vass, J.W. Allison, C.J. Powell, and J.R. Rumble, Jr. NIST X-ray Photoelectron Spectroscopy Database 20, Version 3.5 (National Institute of Standard and Technology, Gaithersburg, MD, 2007); http://srdata.nist.gov/xps/ (accessed December 8, 2010).
34. Z.X. He and W. Pong: X-ray photoelectron spectra of MgH_2. *Phys. Scr*. **41**, 930 (1990).
35. S.J. Splinter, N.S. Mclntyre, W.N. Lennard, K. Griffiths, and G. Palumbo: An AES and XPS study of the initial oxidation of polycrystalline magnesium with water vapour at room temperature. *Surf. Sci*. **292**, 130 (1993).
36. O.G. Ershova, V.D. Dobrovolsky, Y.M. Solonin, O.Y. Khyzhun, and A.Y. Koval: Influence of Ti, Mn, Fe, and Ni addition upon thermal stability and decomposition temperature of the MgH_2 phase of alloys synthesized by reactive mechanical alloying. *J. Alloy. Comp*. **464**, 212 (2008).
37. V.D. Dobrovolsky, S.N. Yendrzheevskaya, A.K. Sinelnichenko, V.V. Skorokhod, and O.Y. Khyzhun: Analysis of the surface condition of $Ti_4Fe_2O_x$. *Int. J. Hydrogen Energy* **21**, 1061 (2011).